

# Modelling and Simulation of High Pressure Processes in Food Engineering

Sixto Jesús Álvarez<sup>(1)</sup>, Juan–Antonio Infante<sup>(2)</sup>, Benjamin Ivorra<sup>(2)</sup>,  
Ángel Manuel Ramos<sup>(2)</sup> y José María Rey<sup>(1)</sup>

(1) Departamento de Matemática Aplicada  
Facultad de Ciencias Químicas  
Universidad Complutense de Madrid  
Plaza de Ciencias, 3, 28040–Madrid, Spain

e–mail: [sixtoj\\_alvarez@mat.ucm.es](mailto:sixtoj_alvarez@mat.ucm.es), [jose\\_rey@mat.ucm.es](mailto:jose_rey@mat.ucm.es)

web: <http://www.mat.ucm.es/momat>

(2) Departamento de Matemática Aplicada  
Facultad de Ciencias Matemáticas  
Universidad Complutense de Madrid  
Plaza de Ciencias, 3, 28040–Madrid, Spain

e–mail: [ja\\_infante@mat.ucm.es](mailto:ja_infante@mat.ucm.es), [benjamin.ivorra@mat.ucm.es](mailto:benjamin.ivorra@mat.ucm.es), [angel@mat.ucm.es](mailto:angel@mat.ucm.es)

web: <http://www.mat.ucm.es/momat>

April 23, 2007

**Keywords:** Modelization, Food Technology, High Pressure, Heat and Mass Transfer, Microorganism Inactivation, Simulation.

## Abstract

High Pressure (HP) has turned out to be very effective in order to prolong the useful life of some food. This paper deals with the modelling and simulation of the effect of the combination of high pressure with thermal treatments on the food, considering the microbiological inactivation that eventually can take place on certain microorganisms. This is very important in order to be able to design suitable industrial equipments and optimize the processes.

## 1 INTRODUCTION

At present, the demand of safe and minimally processed food, prepared for immediate consumption (ready–to–use and ready–to–eat) has increased significantly, in order to give service to the needs of the sector of the restoration, collective dining rooms (colleges, companies, hospitals, residences, ...) as well as to the domestic consumption.

One of the technologies that can be used for the preparation of these products is High Pressure (HP), which has turned out to be very effective in order to prolong the useful life of some food (cooked ham, juices, guacamole, oysters, ...) being already a reality at industrial level. These treatments have the great advantage of not being based on the incorporation of additives, which consumers prefer to elude. Furthermore, they allow to avoid the treatments with high temperatures (as the Pasteurization), which have adverse effects on some nutritional properties of the food, its flavor, ...

This paper deals with the modelling and simulation of the effect of the combination of high pressure with thermal treatments on the food, considering the microbiological inactivation that eventually can take

place on certain microorganisms. This is very important in order to be able to design suitable industrial equipments and optimize the processes.

In Section 2 some models for microorganism inactivation are presented. These models need pressure and temperature as an input. These quantities are obtained by means of the models developed in Section 3. In Section 4 we couple those models in order to get numerical results for the distribution of temperature and inactivation of microorganisms. Finally, in Section 8 we expose the final remarks, proposing several steps to follow in order to optimize a thermal–HP process for a particular food and equipment.

## 2 MICROORGANISM INACTIVATION

One of the main objectives of the HP–Thermal treatments is to decrease some undesirable biological activities (enzymatic reactions, bacterial contamination, ...) keeping safe other properties of the processed food (vitamins, color, taste, ...). In order to predict the impact of our treatment on the biological activities inside the considered food sample, we introduce and describe a particular first order kinetic model. Basically, this model describes the activity evolution in function of the pressure–temperature evolution. The coefficients involved in the model are determined by using experimental measurements.

### 2.1 Experimental measurement of the activity

In practice, there are several ways to define and measure the activity of a biological entity. However, it essentially depends on the kind of entity considered and generally follows the following two steps [1, 2, 3]:

1. Definition of the kind of activity which is studied (for example: the amount of catalysis reaction if we study an enzyme, the reproduction velocity if we consider a bacteria, ...).
2. Choice of the experimental protocol used to measure the considered activity (optical density variation, chemical reaction, ...).

Once those steps are performed the considered biological activity at a particular pressure–temperature condition may be experimentally measured.

### 2.2 Mathematical model for microorganism inactivation

The evolution of the activity  $A$  of a biological entity is often described by the following first-order kinetic equation [4, 5]:

$$\frac{dA(t)}{dt} = -k(P(t), T(t)) A(t), \quad (1)$$

where  $t$  is the time (min),  $P(t)$  is the pressure (MPa) at time  $t$ ,  $T(t)$  is the temperature (K) at time  $t$  and  $k(P(t), T(t))$  is the inactivation rate ( $\text{min}^{-1}$ ).

There exist various mathematical equations describing  $k(P, T)$ , all based on equations modelling pressure–temperature dependence of chemical reactions. Each version is adapted to a particular biological entity. Here we limit the exposition to two equations which are used for numerical simulations in Section 4:

- An equation provided by the association of the the Arrhenius equation (modelling the temperature dependence) and the Eyring equation (modelling the pressure dependence) [1]:

$$k(P, T) = k_{\text{ref}} \exp \left( -B \left( \frac{1}{T} - \frac{1}{T_{\text{ref}}} \right) \right) \exp(-C(P - P_{\text{ref}})) \quad (2)$$

where  $T_{\text{ref}}$  is a reference temperature (K),  $P_{\text{ref}}$  is a reference pressure (MPa),  $k_{\text{ref}}$  is the inactivation rate at reference conditions ( $\text{min}^{-1}$ ),  $B$  is the parameter expressing the temperature dependence of  $k$  (K) and  $C$  is the parameter expressing the pressure dependence of  $k$  ( $\text{MPa}^{-1}$ ).

- A model obtained by considering the transition state theory of Eyring and particularly well adapted to the enzyme study [2, 3]:

$$k(P, T) = k_{\text{ref}} \exp\left(\frac{-\Delta V_{\text{ref}}}{RT}(P - P_{\text{ref}})\right) \exp\left(\frac{\Delta S_{\text{ref}}}{RT}(T - T_{\text{ref}})\right) \exp\left(\frac{\Delta \kappa}{2RT}(P - P_{\text{ref}})^2\right) \exp\left(\frac{-2\Delta \zeta}{RT}(P - P_{\text{ref}})(T - T_{\text{ref}})\right) \exp\left(\frac{\Delta C_p}{RT}\left(T\left(\ln \frac{T}{T_{\text{ref}}}\right) - 1\right) + T_{\text{ref}}\right) + \text{high order terms}, \quad (3)$$

where  $R = 8.314 \text{ (J mol}^{-1}\text{K}^{-1}\text{)}$  is the universal gas constant,  $\Delta V_{\text{ref}}$  is the volume change at reference conditions ( $\text{cm}^3 \text{ mol}^{-1}$ ),  $\Delta S_{\text{ref}}$  is the entropy change at reference conditions ( $\text{J mol}^{-1}\text{K}^{-1}$ ),  $\Delta C_p$  is the heat capacity change ( $\text{J mol}^{-1}\text{K}^{-1}$ ),  $\Delta \kappa$  is the compressibility factor ( $\text{cm}^6 \text{ J}^{-1} \text{ mol}^{-1}$ ) and  $\Delta \zeta$  is the thermal expansibility factor ( $\text{cm}^3 \text{ mol}^{-1}\text{K}^{-1}$ ). Depending of the studied enzyme, higher order terms can be added to (3) in order to refine the approximation of the pressure temperature dependence of the activity [3].

The parameters of the selected equation are estimated using regression techniques on data provided by experimental measurements of the activity [6].

Once the equation and parameters of  $k$  are obtained, the solution at time  $t$  of (1) is given by

$$A(t) = A(0) \exp\left(-\int_0^t k(P(\tau), T(\tau)) d\tau\right). \quad (4)$$

These models have been successfully applied to the study of the inactivation of various enzymes with different conditions of pressure and temperature (see [1, 2, 3]).

### 3 HEAT AND MASS TRANSFER MODELLING

When HP is applied in Food Technology, it is necessary to consider thermal effects produced by variations of temperature due to the work of compression/expansion in both the food and the pressurizing fluid.

These variations of temperature are different in the sample of food and the pressurizing medium due to their different nature and compression heating. Consequently the medium can heat/cool the sample and a transfer of heat appears.

After compression, heat exchange appears between the walls of the pressure chamber, the pressure medium and the packaged food giving a time-dependent distribution of temperatures. In the fluid media (the pressurizing fluid and also the food when it is in liquid state) changes in temperatures imply changes in fluid density leading to free convection during the high pressure process. Therefore, conduction and convection has been considered in the models, taking into account heat and mass transfer.

Often, HP experiments are carried out in a cylindrical pressure vessel previously (typically a hollow steel cylinder) filled with the food and the pressure medium. The sample is located in the inner chamber at some temperature that can be the same or different than the pressure medium and/or the solid walls surrounding it which may cool or warm the food following user's criteria.

By axial symmetry, we may consider cylindrical coordinates and the domain given by half a cross section (intersection of the cylinder with a plane containing the axis). Then, we consider four bidimensional sub-domains:

- $\Omega_F$ , representing the domain where the sample of food is located.
- $\Omega_C$  is the cap of the sample holder (typically a rubber cap).
- $\Omega_P$ , representing the domain occupied by the pressurizing medium.
- $\Omega_S$ , representing the domain of the steel walls surrounding the above domains.

Then, our domain in the  $(r, z)$ -coordinates (see Figure 1) is the rectangle  $\Omega = [0, L] \times [0, H]$  defined by

$$\overline{\Omega} = \overline{\Omega_F \cup \Omega_C \cup \Omega_P \cup \Omega_S}$$

In the boundary of  $\Omega$ , which is denoted by  $\partial\Omega$ , we distinguish

- $\Gamma_r \subset \{L\} \times (0, H)$ , where the temperature will be fixed, and
- $\Gamma_{up} = [0, L] \times \{H\}$ , where a small transfer of heat with the room where the equipment is located could take place.

We denote by  $\Omega^*$ ,  $\Omega_F^*$ ,  $\Omega_C^*$ ,  $\Omega_P^*$ ,  $\Omega_S^*$ ,  $\Gamma_r^*$  and  $\Gamma_{up}^*$  to the domains generated when rotating  $\Omega$ ,  $\Omega_F$ ,  $\Omega_C$ ,  $\Omega_P$ ,  $\Omega_S$ ,  $\Gamma_r$  and  $\Gamma_{up}$  along the axis of symmetry (in the 3D space).

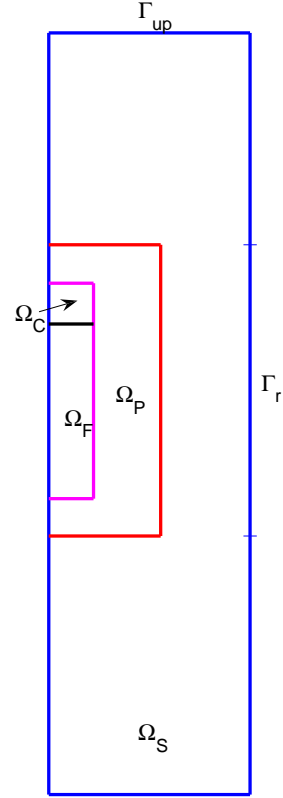


Figure 1: Computational domain

### 3.1 Solid type foods

#### 3.1.1 Heat transfer by conduction

When solid type foods are considered, the starting point is the heat conduction equation for the temperature  $T$  (K)

$$\rho C_p \frac{\partial T}{\partial t} - \nabla \cdot (k \nabla T) = \alpha \frac{dP}{dt} T \text{ in } (0, t_f) \times \Omega^*, \quad (5)$$

where  $\rho$  is the density (kg/m<sup>3</sup>),  $C_p$  is the heat capacity (J/kg K),  $k$  is the thermal conductivity (W/mK) and  $t_f$  is the final time. The right hand side is the internal heat generation, due to the change of pressure (see [7]) where  $P = P(t)$  represents the pressure (Pa) applied by the equipment (this is chosen by the user within the machine limitations) and  $\alpha$  is given by

$$\alpha = \begin{cases} \text{thermal expansion coefficient (K}^{-1}\text{) of the food in } \Omega_F^*, \\ \text{thermal expansion coefficient (K}^{-1}\text{) of the pressure fluid in } \Omega_P^*, \\ 0, \text{ elsewhere.} \end{cases}$$

This term results from the following law:

$$\frac{\Delta T}{\Delta P} = \frac{\alpha \cdot T \cdot V}{M \cdot C_p} = \frac{\alpha \cdot T}{\rho \cdot C_p},$$

where  $\Delta T$  is the change of temperature due to a change of pressure  $\Delta P$ ,  $V$  ( $\text{m}^3$ ) is the volume and  $M$  (kg) is the mass. Therefore, we obtain

$$\rho \cdot C_p \cdot \Delta T = \alpha \cdot T \cdot \Delta P.$$

We point out that if we want to use temperatures in  $^{\circ}\text{C}$  instead of  $^{\circ}\text{K}$  we only have to change  $T$  by  $T + 273.15$  in the right hand side of equation (5).

In order to have a unique solution, the conduction heat transfer equation (5) is completed with appropriate boundary and initial conditions:

$$\begin{cases} k \frac{\partial T}{\partial \mathbf{n}} = 0 & \text{on } \partial\Omega^* \setminus (\Gamma_r^* \cup \Gamma_{\text{up}}^*), \\ k \frac{\partial T}{\partial \mathbf{n}} = h(T_{\text{amb}} - T) & \text{on } \Gamma_{\text{up}}^*, \\ T = T_{\text{ref}} & \text{on } \Gamma_r^*, \\ T(0) = T_0 & \text{in } \Omega^*, \end{cases} \quad (6)$$

where  $\mathbf{n}$  is the outward normal vector on the boundary of the domain,  $T_{\text{ref}}$  and  $T_{\text{amb}}$  are the temperatures that are kept constant in  $\Gamma_R^*$  (cooling or warming the food sample) and at the external ambient, respectively, and  $h$  ( $\text{W m}^{-2}\text{K}^{-1}$ ) is the heat transfer coefficient.

By using cylindrical coordinates, system (5)–(6) can be rewritten as the following 2D problem:

$$\begin{cases} \rho C_p \frac{\partial T}{\partial t} - \frac{1}{r} \frac{\partial}{\partial r} \left( r k \frac{\partial T}{\partial r} \right) - \frac{\partial}{\partial z} \left( k \frac{\partial T}{\partial z} \right) = \alpha \frac{dP}{dt} T & \text{in } (0, t_f) \times \Omega, \\ k \frac{\partial T}{\partial \mathbf{n}} = 0 & \text{on } (0, t_f) \times \partial\Omega \setminus (\Gamma_r \cup \Gamma_{\text{up}}), \\ k \frac{\partial T}{\partial \mathbf{n}} = h(T_{\text{amb}} - T) & \text{on } (0, t_f) \times \Gamma_{\text{up}}, \\ T = T_{\text{ref}} & \text{on } (0, t_f) \times \Gamma_r, \\ T(0) = T_0 & \text{in } \Omega. \end{cases} \quad (7)$$

This model is suitable when the filling ratio of the food inside the vessel is big compared with that of the pressure medium. This has been showed in [7], where the model has been validated with several comparisons between the numerical and experimental results. Nevertheless, in [7] is also showed that, when the filling ratio of the food inside the vessel is not big compared with that of the pressure medium, the solution of this model is far from the experimental measurements. Two ways of solving that inconvenience are the following:

1. We can use the same model but with an apparent conductivity for the pressure medium bigger than the real one. This method will not result in good temperature distributions in the pressure fluid but can give good results inside the food. We will not discuss this possibility in this paper.
2. We can improve the model by including the convection phenomenon that is taking place in the pressure medium. The resulting model is more expensive from a computational point of view but the results are more accurate. We discuss this methodology in Section 3.1.2.

### 3.1.2 Heat transfer by conduction and convection

The inhomogeneous temperature distribution induces an inhomogeneous density distribution in the pressure medium and consequently a buoyancy fluid motion. In other words, free convection.

This fluid motion may strongly influence the temperature distribution. Therefore, if we want to take into account this fact, we need to include the transfer of heat due to convection in the model by adding the term

$$\rho C_p \mathbf{u} \cdot \nabla T$$

to the left hand side of the heat transfer equation. Here  $\mathbf{u}$  (m/s) is the fluid velocity field, which must satisfy the momentum and the continuity equations. Therefore, the system of equations we have included in the model are

$$\left\{ \begin{array}{ll} \rho C_p \frac{\partial T}{\partial t} - \nabla \cdot (k \nabla T) + \rho C_p \mathbf{u} \cdot \nabla T = \alpha \frac{dP}{dt} T & \text{in } (0, t_f) \times \Omega^*, \\ \rho \frac{\partial \mathbf{u}}{\partial t} - \nabla \cdot \eta (\nabla \mathbf{u} + \nabla \mathbf{u}^t) + \rho (\mathbf{u} \cdot \nabla) \mathbf{u} & \\ \quad \quad \quad = -\nabla p - \nabla \cdot \left( \frac{2\eta}{3} (\nabla \cdot \mathbf{u}) I \right) - \rho \mathbf{g} & \text{in } (0, t_f) \times \Omega_P^*, \\ \frac{\partial \rho}{\partial t} + \nabla \cdot (\rho \mathbf{u}) = 0 & \text{in } (0, t_f) \times \Omega_P^*, \end{array} \right. \quad (8)$$

where  $\mathbf{g}$  is the gravity vector (m/s<sup>2</sup>),  $\eta$  is the dynamic viscosity (Pa s),  $P = P(t)$  is the pressure (Pa) applied by the equipment (this is chosen by the user within the machine limitations) and  $P + p$  is the total pressure (Pa) in the pressure medium  $\Omega_P^*$ , with  $p = p(x, t)$  the pressure generated by the mass transfer inside the fluid.

We point out that in the right hand side of the first equation of (8) we could have written  $\alpha \frac{d(P+p)}{dt} T$ , but we have suppose that the internal heat generation due to the mass transfer is negligible. In the right hand side of the second equation of (8) we have written  $\nabla p$  since  $P = P(t)$  depends only on time and therefore  $\nabla(P + p) = \nabla p$ .

In the above equations the density of the pressure medium is suppose to be a known function of  $T$  (i.e.,  $\rho = \rho(T)$ ). Parameters  $k$ ,  $\eta$ ,  $\alpha$  and  $C_p$  can be also considered as known functions of  $T$ .

System (8) is completed with appropriate boundary and initial conditions. Furthermore, in order to be able to get a unique solution we set  $p = 0$  in some corner point CP of  $\partial\Omega_P^*$ .

$$\left\{ \begin{array}{ll} k \frac{\partial T}{\partial \mathbf{n}} = 0 & \text{on } (0, t_f) \times \partial\Omega^* \setminus (\Gamma_r^* \cup \Gamma_{up}^*), \\ k \frac{\partial T}{\partial \mathbf{n}} = h(T_a - T) & \text{on } (0, t_f) \times \Gamma_{up}^*, \\ T = T_{\text{ref}} & \text{on } (0, t_f) \times \Gamma_r^*, \\ \mathbf{u} = 0 & \text{on } (0, t_f) \times \partial\Omega_P^*, \\ T(0) = T_0 & \text{in } \Omega^*, \\ p = 0 & \text{in } (0, t_f) \times \text{CP}. \end{array} \right. \quad (9)$$

As showed in Section 3.1.1 for the conduction heat transfer model (see system (7)), system (8)–(9) can be rewritten as an equivalent 2D problem by using cylindrical coordinates (we do not write the resulting system).

This model is suitable independently of the filling ratio of the food inside the vessel. This has been showed in [7], where this model (but without the term  $-\nabla \cdot \left( \frac{2\eta}{3} (\nabla \cdot \mathbf{u}) I \right)$  in the second equation of System (8)) has been validated with several comparisons between the numerical and experimental results.

### 3.2 Liquid foods

For liquid foods we must consider convection also in the region  $\Omega_F$  and distinguish two separated velocity fields  $\mathbf{u}_F$  and  $\mathbf{u}_P$  for the food and the pressurizing fluid respectively. We point out that the pressure medium and the food are separated by the sample holder and do not mix.

#### 3.2.1 Governing equations

The governing equations are

$$\left\{ \begin{array}{ll} \rho C_p \frac{\partial T}{\partial t} - \nabla \cdot (k \nabla T) + \rho C_p \mathbf{u} \cdot \nabla T = \alpha \frac{dP}{dt} T & \text{in } (0, t_f) \times \Omega^*, \\ \rho \frac{\partial \mathbf{u}_F}{\partial t} - \nabla \cdot \eta (\nabla \mathbf{u}_F + \nabla \mathbf{u}_F^t) + \rho (\mathbf{u}_F \cdot \nabla) \mathbf{u}_F & \\ \quad \quad \quad = -\nabla p - \nabla \cdot \left( \frac{2\eta}{3} (\nabla \cdot \mathbf{u}) I \right) - \rho \mathbf{g} & \text{in } (0, t_f) \times \Omega_F^*, \\ \rho \frac{\partial \mathbf{u}_P}{\partial t} - \nabla \cdot \eta (\nabla \mathbf{u}_P + \nabla \mathbf{u}_P^t) + \rho (\mathbf{u}_P \cdot \nabla) \mathbf{u}_P & \\ \quad \quad \quad = -\nabla p - \nabla \cdot \left( \frac{2\eta}{3} (\nabla \cdot \mathbf{u}) I \right) - \rho \mathbf{g} & \text{in } (0, t_f) \times \Omega_P^*, \\ \frac{\partial \rho}{\partial t} + \nabla \cdot (\rho \mathbf{u}_F) = 0 & \text{in } (0, t_f) \times \Omega_F^*, \\ \frac{\partial \rho}{\partial t} + \nabla \cdot (\rho \mathbf{u}_P) = 0 & \text{in } (0, t_f) \times \Omega_P^*, \end{array} \right.$$

with point, boundary and initial conditions:

$$\left\{ \begin{array}{ll} k \frac{\partial T}{\partial \mathbf{n}} = 0 & \text{on } (0, t_f) \times \partial \Omega^* \setminus (\Gamma_r^* \cup \Gamma_{up}^*), \\ k \frac{\partial T}{\partial \mathbf{n}} = h(T_a - T) & \text{on } (0, t_f) \times \Gamma_{up}^*, \\ T = T_{ref} & \text{on } (0, t_f) \times \Gamma_r, \\ \mathbf{u}_F = 0 & \text{on } (0, t_f) \times \partial \Omega_F^*, \\ \mathbf{u}_P = 0 & \text{on } (0, t_f) \times \partial \Omega_P^*, \\ T = T_0 & \text{in } \Omega^*, \\ p = 0 & \text{in } (0, t_f) \times CP_F^*, \\ p = 0 & \text{in } (0, t_f) \times CP_P^*, \end{array} \right.$$

where  $CP_F^*$  and  $CP_P^*$  are corner points of  $\partial \Omega_F^*$  and  $\partial \Omega_P^*$ , respectively.

#### 3.2.2 Numerical tests

For the numerical cases we have used the dimensions of the pilot unit (ACB GEC Alsthom, Nantes, France) that was used in [7]. Therefore, the 2D domain has a diameter of 0.1 m diameter and a height of 0.3 m.

Following the cases studied for the solid food type (see Sections 3.1.1 and 3.1.2) we consider two examples of liquid food: a sample with a big filling ratio and a small one. The dimensions and location of the sample in both cases is exactly the same as in the big and small cases studied in [7] for solid type foods.

For the sake of simplicity, the physical parameters of the liquid food and the pressurizing medium are supposed to be equal and depending on temperature (they could be also dependent on pressure). Thermophysical properties of the steel and the rubber cap of the sample holder were considered to be constant.

We present numerical tests computed in cylindrical coordinates with the comercial package COMSOL Multiphysics 3.3a, according to the following choices of parameters (all temperatures  $T$  in expressions below are in  $^{\circ}\text{C}$ ):

$$\rho = \rho(T) = \begin{cases} -0.517 T + 1183 & \text{in } \Omega_F \cup \Omega_P, \\ 1110 & \text{in } \Omega_C, \\ 7833 & \text{in } \Omega_S = \Omega \setminus \{\Omega_F \cup \Omega_P \cup \Omega_C\}, \end{cases}$$

$$C_p = C_p(T) = \begin{cases} -2.8811 \cdot 10^{-5} T^4 + 0.0064805 T^3 - 0.56565 T^2 + 21.534 T + 3499.4 & \text{in } \Omega_F \cup \Omega_P, \\ 1884 & \text{in } \Omega_C, \\ 465 & \text{in } \Omega_S, \end{cases}$$

$$k = k(T) = \begin{cases} 2.0148 \cdot 10^{-7} T^3 - 3.7177 \cdot 10^{-5} T^2 + 0.0037895 T + 0.71053 & \text{in } \Omega_F \cup \Omega_P, \\ 0.173 & \text{in } \Omega_C, \\ 55 & \text{in } \Omega_R, \end{cases}$$

$$\alpha = \alpha(T) = -1.9784 \cdot 10^{-7} T + 0.00045271,$$

$$\eta = \eta(T) = -3.7287 \cdot 10^{-9} T^3 + 7.1227 \cdot 10^{-7} T^2 - 5.5079 \cdot 10^{-5} T + 0.0022029 \text{ in } \Omega_F \cup \Omega_P,$$

$$T_{\text{amb}} = 19.3^{\circ}\text{C} \text{ and } h = 28.$$

Numerical experiments simulate the temperature evolution starting from  $T_0 = 22^{\circ}\text{C}$  and  $T_0 = 40^{\circ}\text{C}$ , respectively, when a high pressure treatment is applied, and when  $T_{\text{ref}} = 40^{\circ}\text{C}$  is chosen. For each one of this cases we compute the solution for the big and the small food sample and show the evolution of the temperature during 15 minutes, also in two cases:

1. A constant pressure increase in the first 183 seconds until reach 360 MPa is considered. Therefore, the derivative of pressure in the internal heat generation is

$$\frac{dP}{dt} = \begin{cases} \frac{360 \cdot 10^6}{183}, & 0 < t \leq 183, \\ 0, & t > 183. \end{cases}$$

2. Applying the same constant pressure increase in the first 305 seconds until reaching 600 MPa. In this case

$$\frac{dP}{dt} = \begin{cases} \frac{600 \cdot 10^6}{305}, & 0 < t \leq 305, \\ 0, & t > 305. \end{cases}$$

Therefore we show results for eight different numerical experiments. At this moment, we do not have experimental data available to validate the model (which is part of our future work).

Figure 2 shows the evolution of the temperature in the big sample at two points: the first one is located at the center of the sample (over the symmetry axis) and the second one is over the surface of the sample. In that figure, the four treated cases, for different initial temperature and pressure, are considered. Figure 3 show an analogous graphic for the small sample.



The temperature distribution for the small sample at the final time ( $t = 15$  min) is shown in Figure 4.

As already remarked in [7] for solid type foods, these results show that for liquid foods it can be also interesting to use an initial temperature for the food smaller than  $T_{\text{ref}}$  in order to anticipate the temperature increase resulting from compression, which allows to get a more uniform process avoiding big temperature gradients inside the food and temperatures much higher than  $T_{\text{ref}}$  (we remember that one of the goals of the high-pressure technology is to process the food without using high temperatures, which degrade some of the main qualities of the food).

### 3.2.3 Identification of parameters

One of the critical points in the modelling is the choice of the value of the parameters to be used in the models.

Accurate thermophysical properties (pressure and temperature dependent), of food and pressure medium can be obtained from those corresponding to pure water (see, e.g., [8] [9] and the references therein) when they are close to water.

For general cases, identification of these parameters by means of mathematical tools for inverse problems can be needed. In [10] the authors discuss how to identify the heat transfer coefficient for a particular prototype.

## 4 MICROORGANISM INACTIVATION AND HEAT-MASS TRANSFER

In this Section we present a numerical study of the impact of various HP-Thermal treatments on the inactivation of three different enzymes: Bacillus Subtilis  $\alpha$ -Amylase, Lipoxygenase, and Carrot Pectin Methyl-Estarase. In order to do that, we couple the heat transfer model presented in Section 3.2 for liquid foods with the kinetic equation (1), where  $k$  is chosen between (2) or (3) depending on the enzyme. Similar results can be obtained for the models presented in Section 3.1 for solid type foods.

## 5 Inactivation model implementation for considered enzymes

**Bacillus Subtilis  $\alpha$ -Amylase (BSAA):** It is an enzyme produced by a bacteria called Bacillus subtilis. This bacteria, present in the ground, can contaminate aliment and in rare occasion cause intoxications. This enzyme catalyze the hydrolisis of starch generating sugars (as maltose), which can modify the taste of the aliment.

The inactivation rate  $k$  is modelled using equation (2) with  $P_{\text{ref}} = 500$  MPa,  $T_{\text{ref}} = 313$  K,  $k_{\text{ref}} = 9.2 \times 10^{-2} \text{ min}^{-1}$ ,  $B = 10097$  K and  $C = -8.7 \times 10^{-4} \text{ MPa}^{-1}$ . Interested reader can found more detail about the experimental protocol and the parameters determination in [1].

**Lipoxygenase (LOX):** This enzyme is present in various plants and vegetables such as green beans and green peas. It is responsible of the apparition of undesirable aromas in those aliments. During this work we study the inactivation of this enzyme into green bean juice.

Equation (3) is used to describe  $k$  with  $P_{\text{ref}} = 500$  MPa,  $T_{\text{ref}} = 298$  K,  $k_{\text{ref}} = 1.34 \times 10^{-2} \text{ min}^{-1}$ ,  $\Delta V_{\text{ref}} = -308.14 \text{ cm}^3/\text{mol}$ ,  $\Delta S_{\text{ref}} = 90.63 \text{ J mol}^{-1} \text{ K}^{-1}$ ,  $\Delta C_p = 2466.71 \text{ J mol}^{-1} \text{ K}^{-1}$ ,  $\Delta \zeta = 2.22 \text{ cm}^3 \text{ mol}^{-1} \text{ K}^{-1}$ ,  $\Delta \kappa = -0.54 \text{ cm}^6 \text{ J}^{-1} \text{ mol}^{-1}$  (see [2] for more details).

**Carrot Pectin Methyl-Estarase (CPE):** Pectinesterase is an enzyme common in most of vegetables. It can be present in vegetable juices and in this case it deesterifies pectin, producing low-methoxyl pectin. This deesterification reduces juice viscosity and the presence of low-methoxyl pectin generates

cloud loss (affecting juice flavor, color, texture and aroma). Here we concentrate on the Pectinesterase present in carrot juice (Carrot Pectin Methyl–Estarase).

For Carrot Pectin Methyl–Estarase we apply equation (3) to model  $k$  with  $P_{\text{ref}} = 700 \text{ MPa}$ ,  $T_{\text{ref}} = 323.15 \text{ K}$ ,  $k_{\text{ref}} = 7.05 \times 10^{-2} \text{ min}^{-1}$ ,  $\Delta V_{\text{ref}} = -44.0124 \text{ cm}^3 \text{ mol}^{-1}$ ,  $\Delta S_{\text{ref}} = 168.4 \text{ J mol}^{-1} \text{ K}^{-1}$ ,  $\Delta C_p = 1376.6 \text{ J mol}^{-1} \text{ K}^{-1}$ ,  $\Delta \zeta = -0.0339 \text{ cm}^6 \text{ J}^{-1} \text{ mol}^{-1}$ ,  $\Delta \kappa = -0.1195 \text{ cm}^6 \text{ J}^{-1} \text{ mol}^{-1}$  (see [3]).

## 6 High Pressure–Temperature treatments studied

We consider the heat transfer model presented in Section 3.2 (for liquid foods) applied to a big and a small food sample. For both cases we consider the two following high pressure temperature treatments:

- Treatment denoted by T1: A treatment of 15 min with a sample initial temperature of 22°C and a final pressure of 600 MPa.
- Treatment denoted by T2: A treatment of 15 min with a sample initial temperature of 40°C and a final pressure of 360 MPa.

The objective is to compare the efficiency of using higher pressures or higher temperatures during the treatment.

## 7 Numerical Results

Temperature range and final average enzymatic activity reduction reached during simulation are reported on Table 1. For each case, the time evolution of the average enzyme activity is depicted in Figure 5. The distribution of enzyme activity and temperature at final time (15 min) is presented in Figure 6 for a big food sample with treatment T2.

As we can observe on Table 1, the efficiency of treatment T1 and T2 depends of the considered enzyme:

- For BSAA, T2 is a little more efficient. However the difference between T1 and T2 in the small sample case (+4%) is less important than the big sample case (+11%). This is due to the fact that the average sample temperature for T2 is more elevated.
- For LOX, T1 is clearly the more appropriated. In both sample size cases, this treatment is three times more efficient than the T2 treatment. This enzyme is more sensible to high pressure.
- For CPE, T1 and T2 are equivalents (with a little advantage for T2). This enzyme seems to be resistant to both treatments. We generally obtain a reduction of only 15%.

However in all cases, we can remark that the final temperature and enzymes activity distributions are generally in adequation: warmer is a zone, lower is the activity.

Analyzing results obtained with those three enzymes, we can not privilege one of the both treatment. In fact, for each kind of enzyme, we should consider a specific optimal treatment.

## 8 CONCLUDING REMARKS

The mathematical models described in this paper provides a useful tool to design and optimize processes based in the combination of thermal and high pressure processes in Food Technology. They take into account the heat and mass transfer phenomena and the inactivation of microorganisms occurring during the process.

	Min. temp.	Max. Temp.	BSAA a.a.r.	LOX a.a.r.	CPE a.a.r.
T1–Big	22	47	50%	66%	13%
T2–Big	40	54	61%	20%	15%
T1–Small	22	45	47%	68%	12%
T2–Small	40	52	51%	15%	15%

Table 1: Results obtained in big and small sample for each treatment T1 and T2: (**Min. temp.**) Minimum temperature reached in sample, (**Max. Temp.**) maximum temperature reached in sample, BSAA, LOX and CPE average activity reduction (**a.a.r.**) in sample.

The model developed in Section 3.2 for liquids foods has not been validated yet but the results are consistent with what is expected. We intend to carry out this validation soon in a way similar to that of [7] for solid type foods.

Numerical results show that there is not a general optimal treatment. For each particular kind of food and HP equipment we propose to carry out the following steps:

1. Identify the more important microorganisms we want to inactivate and get mathematical models (for each one of them) describing such a process in terms of pressure and temperature (see Sections 2 and 5).
2. Choose a suitable model describing the distribution of temperatures in the food (see Section 3).
3. Use the distribution of temperatures as an input for the kinetic equations describing the inactivation of microorganisms in order to get their final activities after the thermal-HP process (see Section 4).
4. Perform several numerical experiments (changing initial temperature, applied pressure, ...) in order to optimize the process to get temperatures not too high (see Figures 2 and 3), reduction of microorganism activities (see Figures 5, 6 and Table 1), ...

## ACKNOWLEDGEMENTS

This paper was carried out with financial support from the Spanish “Ministerio de Educación y Ciencia” through the AGL2006–12112–C03–02/ALI project and from the “Dirección General de Universidades e Investigación de la Conserjería de Educación de la Comunidad de Madrid” and the “Universidad Complutense de Madrid” in Spain through the CCG06–UCM/ESP–1110 project.

## References

- [1] Linda R. Ludikhuyze, Ilse Van den Broeck, Carla A. Weemaes and Marc E. Hendrickx, Kinetic Parameters for Pressure–Temperature Inactivation of *Bacillus subtilis*  $\alpha$ -Amylase under Dynamic Conditions, *Biotechnol. Prog.*, American Chemical Society and American Institute of Chemical Engineers, Vol. **13**, pp. 617–623 (1997).
- [2] Inneke Indrawati, Linda R. Ludikhuyze, Ann M. Van Loey and Marc E. Hendrickx, Lipxygenase Inactivation in Green Beans (*Phaseolus vulgaris* L.) Due to High Pressure Treatment at Subzero and Elevated Temperatures, *J. Agric. Food Chem.*, American Chemical Society, Vol. **48**, pp. 1850–1859 (2000).
- [3] B. Ly–Nguyen, A. M. Van Loey, C. Smout, S. E. Özcan, D. Fachin, I. Verlent, S. Vu Truong, T. Duvetter and M. E. Hendrickx, Mild–Heat and High–Pressure Inactivation of Carrot Pectin Methylsterase: A Kinetic Study, *Journal of Food Science*, Institute of Food Technologists, Vol. **68**(4), pp. 1377–1383 (2003).

- [4] K. Miyagawa and K. Suzuki, Studies on Taka–amylase *A* under high pressure: Some kinetic aspects of pressure inactivation of Taka–amylase, *A. Arch. Biochem. Biophys.* Vol. **105**, pp. 297–302 (1964).
- [5] K. Suzuki and K. Kitamura, Inactivation of enzyme under high pressure: Studies on the kinetics of inactivation of *R*–amylase of *Bacillus subtilis* under high pressure, *J. Biochem.*, Vol. **54** (3), pp. 214–219 (1963).
- [6] K. D. Dolan, L. Yang and C.P. Trampel, Nonlinear regression technique to estimate kinetic parameters and confidence intervals in unsteady-state conduction-heated foods, *J. Food Eng.*, Vol. **80**, pp. 581–593 (2007).
- [7] L. Otero, Á. M. Ramos, C. de Elvira and P. D. Sanz, A Model to Design High-Pressure Processes Towards an Uniform Temperature Distribution. *J. Food Eng.*, Vol. **78**, pp. 1463–1370, doi:10.1016/j.jfoodeng.2006.01.020 (2007).
- [8] *Thermophysical properties of liquid secondary refrigerants*. A. Melinder ed., *International Institute of Refrigeration*, Paris, (1997).
- [9] L. Otero, A. D. Molina–García and P. D. Sanz, Some interrelated thermophysical properties of liquid water and ice I. A user–friendly modeling review for food high-pressure processing. *Critical Reviews in Food Science and Nutrition*, Vol. **42** (4), pp. 339–352 (2002).
- [10] B. Guignon, Á. M. Ramos, J. A. Infante, J. M. Díaz and P. D. Sanz, Determining thermal parameters in the cooling of a small–scale high pressure freezing vessel. *International Journal of Refrigeration*, Vol. **29**, pp. 1152–1159 (2006).

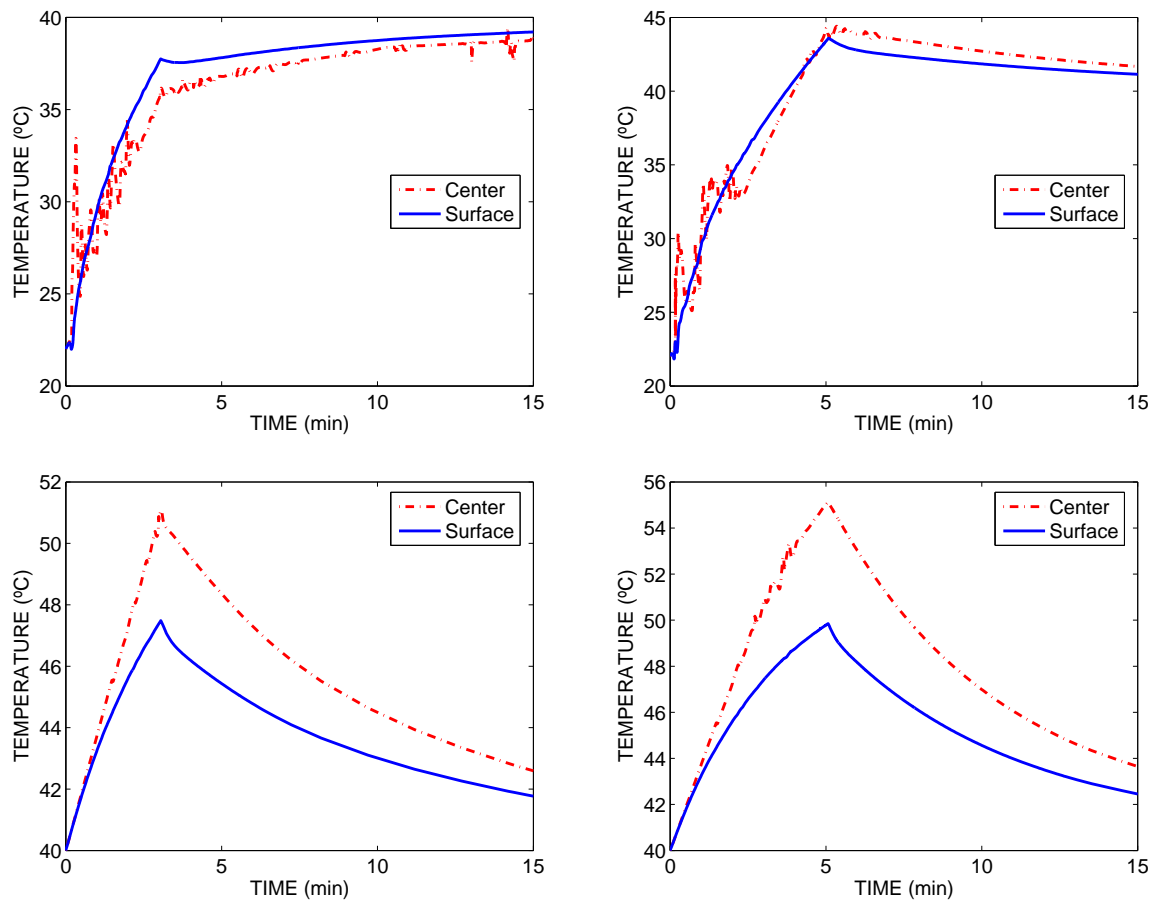


Figure 2: **Big sample:** Evolution of temperature at the center and the surface (left: 360MPa, right: 600MPa, top: initial temperature 22°C, bottom: initial temperature 40°C).

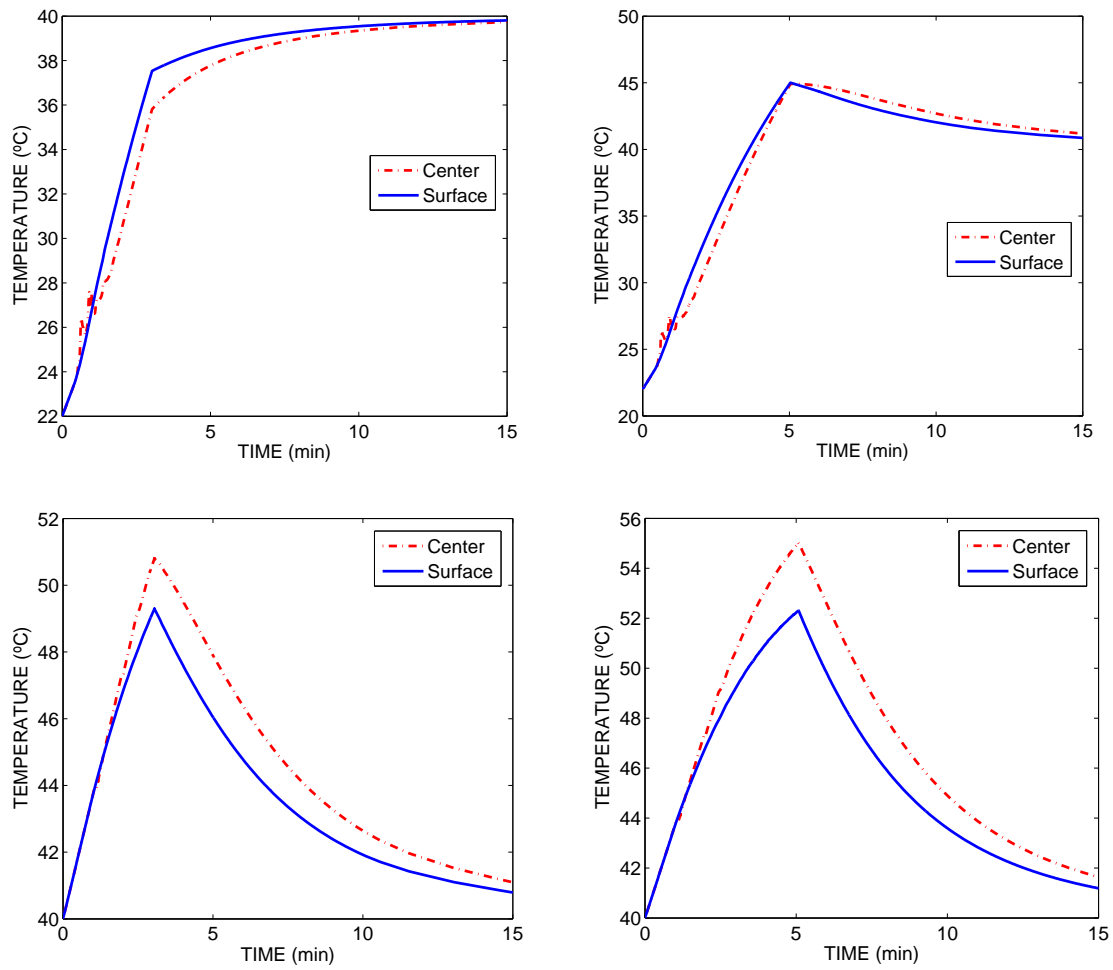
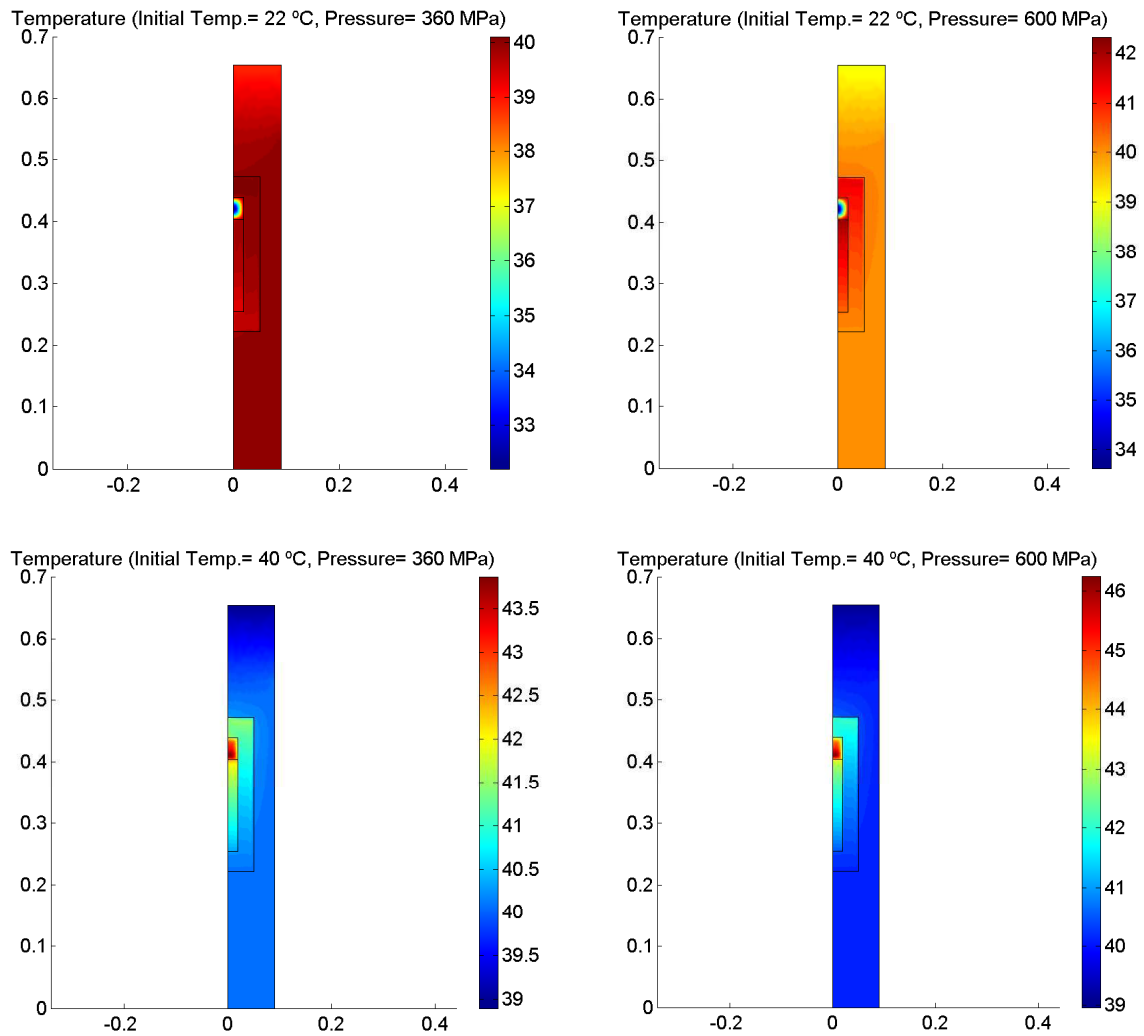


Figure 3: **Small sample:** Evolution of temperature at the center and the surface (left: 360MPa, right: 600MPa, top: initial temperature 22°C, bottom: initial temperature 40°C).

Figure 4: Small sample: Temperature at  $t = 15$  min

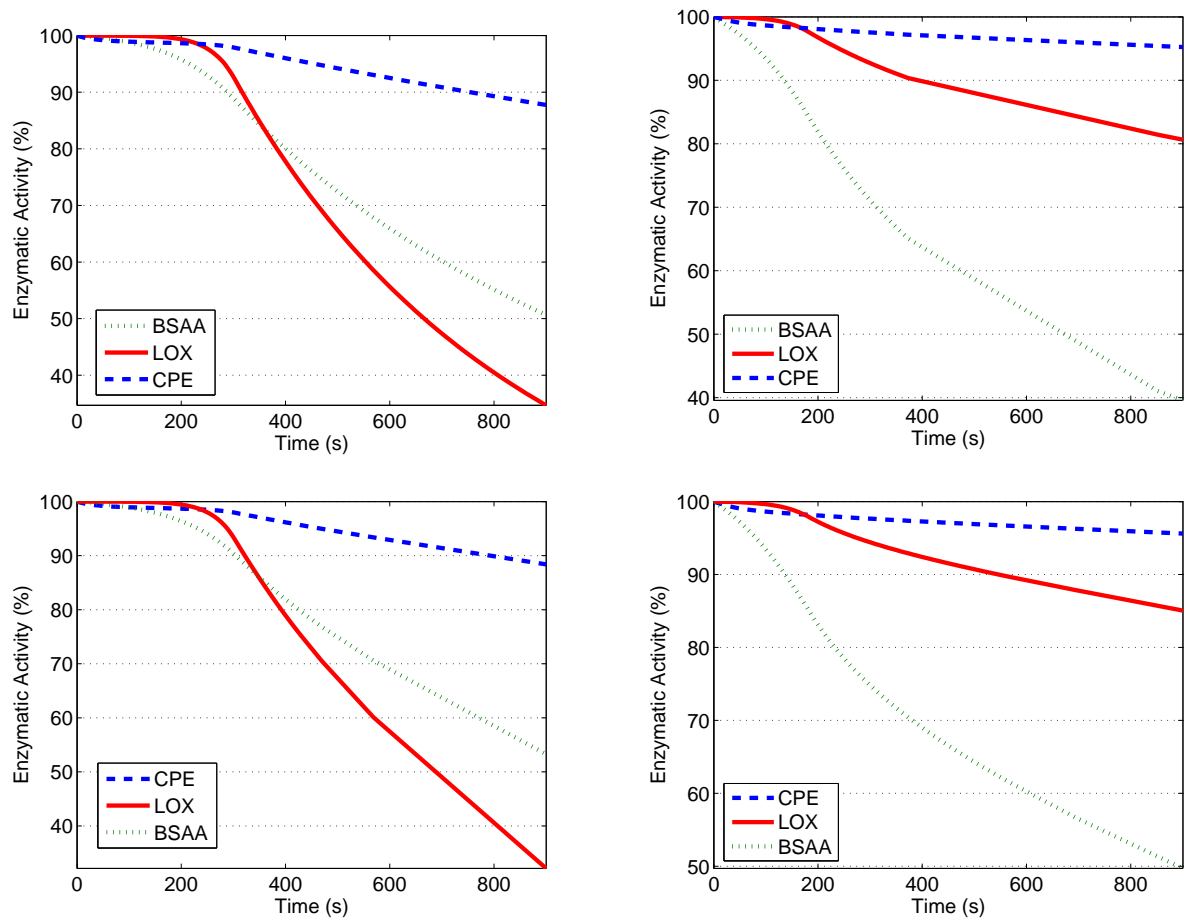


Figure 5: Enzymatic activity evolution for treatment T1 (Left) and T2 (Right) of the big (Top) and small (Bottom) food Sample.



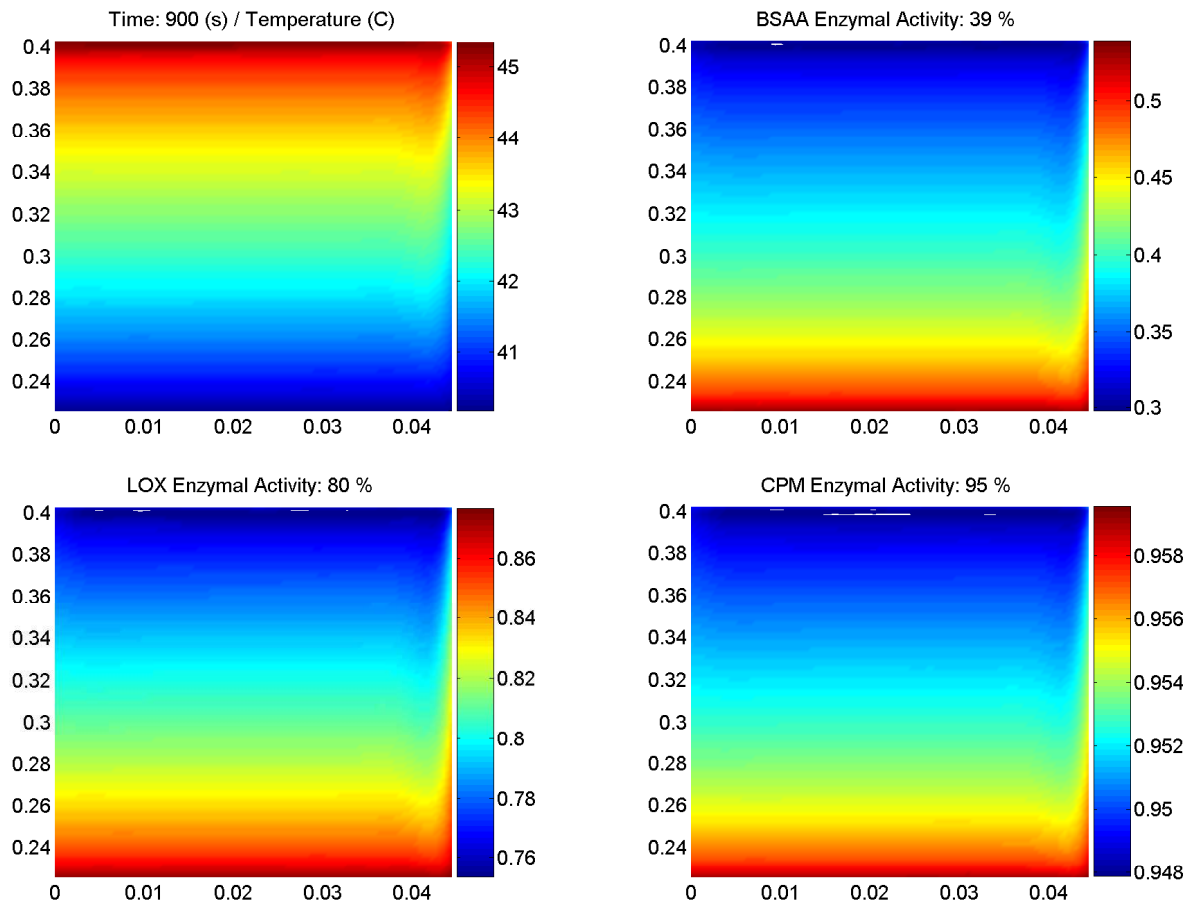


Figure 6: Big food sample with treatment T2. Temperature distribution in the sample at final time (**Top-Left**), BSAA Activity (**Top-Right**), LOX Activity (**Bottom-Left**) and CPE Activity (**Bottom-Right**).